Inorganic Chemistry

Article

pubs.acs.org/IC

Tetra-Armed Cyclen Bearing Two Benzo-15-Crown-5 Ethers in the Side Arms

Mari Ikeda,[†,‡] Mikako Matsumoto,[§] Shunsuke Kuwahara,[‡,§] and Yoichi Habata*[,‡,§]

[†]Education Center, Faculty of Engineering, Chiba Institute of Technology, Shibazono 2-1-1, Narashino, Chiba 275-0023, Japan

[‡]Research Center for Materials with Integrated Properties and [§]Department of Chemistry, Faculty of Science, Toho University, 2-2-1 Miyama, Funabashi, Chiba 274-8510, Japan

Supporting Information

ABSTRACT: A tetra-armed cyclen bearing two benzo-15-crown-5 ethers in the side arms (**1**) is reported. When 1 equiv of Ag^+ is added to **1**, the aromatic side arms cover the Ag^+ incorporated in the cyclen. Upon the addition of more than 1 equiv of Ag^+ to **1**, the cyclen moiety binds Ag^+ first, before the crown ether in the side arms subsequently binds Ag^+. The log K_{11}, log K_{12}, and log K_{13} values for the 1:1, 1:2, and 1:3 (= **1**/Ag^+) complexes were estimated to be 9.4, 5.8, and 4.0, respectively. We found that the tetra-armed cyclen possessing crown ethers in the side arms behaves like an argentivorous molecule even though the crown ether arms bind metal cations.

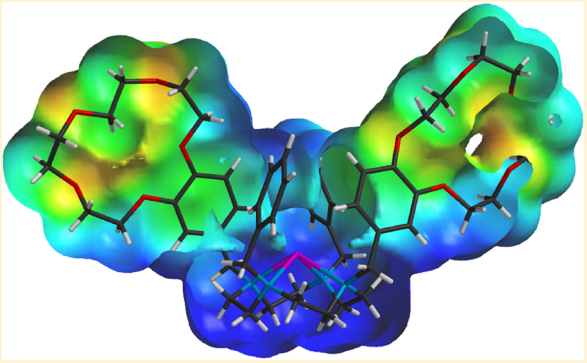

INTRODUCTION

Since the pioneering work of Pedersen on crown ethers,[1] a significant number of macrocyclic compounds have been reported.[2] Recently, hybrid compounds that contain both crown ethers and cyclens in the molecule have received much attention. These compounds have been designed for luminescence emission,[3] anion receptors,[4] DNA-cleavage,[5] anion sensors,[6] fluorescence properties,[7] and recognition of amino acids.[8] Recently, we have reported that tetra- and double-armed cyclens act as argentivorous molecules[9] by Ag^+–π and CH–π interactions.[10] We designed a tetra-armed cyclen bearing two 15-crown-5 ethers in the side arms (**1**) because we want to answer the following questions: (i) when the crown ether moieties in the side arms of the **1**·Ag^+ complex bind metal ions, do the aromatic side arms with metal cations cover the Ag^+ incorporated in the cyclen cavity, and (ii) when the dynamic conformational changes of the side arms occur upon addition of Ag^+, are the binding properties toward the alkali metal cations of the crown ethers in the side arms altered? That is to say, can two crown ethers that bind independently work cooperatively by forming a cyclen·Ag^+ complex? We report herein on the structures and complexing behavior of **1** and the **1**·Ag^+ complex toward alkali metal ions.

RESULTS AND DISCUSSION

Armed-cyclen **1** was prepared in 57% yield by the reaction of 4′-chloromethylbenzo-15-crown-5 ether[9] and 1,7-bisbenzyl-1,4,7,10-tetraazacyclododecane[10c] in the presence of Na_2CO_3 in acetonitrile (Scheme 1). The structure of **1** was confirmed by NMR (^{1}H and ^{13}C NMR, COSY, HOHAHA, and HMQC), fast atom bombardment mass spectrometry (FAB-MS), elemental analysis, and X-ray crystallography [see Supporting Information].

Figure 1 shows the X-ray structure of **1**. In this structure, the cyclen unit forms a chairlike conformation, and the benzene rings cover the crown ether rings. The distances between the benzene planes (C10–C15 (horizontal blue plane in Figure 1c) and C32–C37 (horizontal gray plane in Figure 1c)) and the hydrogen atoms (H52 and H30) are 2.672 and 2.690 Å, respectively. The distances are typical CH–π bond distances.[10]

The stoichiometry of the interaction of Ag^+ with **1** was investigated by cold-spray ionization mass spectrometry (CSI-MS). Figure 2 and Figure S6a–g in the Supporting Information show observed ion peaks and the theoretical ion distributions of 1:0.0, 1:0.5, 1:1.0, 1:1.5, 1:2.0, 1:2.5, and 1:3.0 (= **1**/Ag^+). When 1 equiv of Ag^+ was added, a fragment ion peak arising from $[\mathbf{1} + Ag^+]^+$ was observed. In the cases of 1:2 and 1:3 (= **1**/Ag^+), fragment ion peaks arising from $[\mathbf{1} + 2Ag^+ + CF_3SO_3^-]^+$ appeared. Finally, ion peaks for $[\mathbf{1} + Ag^+]^+$, $[\mathbf{1} + 2Ag^+ + CF_3SO_3^-]^+$, $[\mathbf{1} + 3Ag^+ + 2CF_3SO_3^-]^+$, $[\mathbf{1} + 2Ag^+]^{2+}$, and $[\mathbf{1} + 3Ag + CF_3SO_3^-]^{2+}$ were observed with the correct theoretical ion distributions when 3 equiv of Ag^+ were added. These CSI-MS data suggest that **1** forms 1:1, 1:2, and 1:3 complexes, depending on the stoichiometry between **1** and Ag^+ ions.

Figure 3 shows the X-ray structure of a 1:1 (= **1**/Ag^+) complex. The Ag^+ is four-coordinated by the cyclen nitrogen atoms. The four aromatic side arms cover the Ag^+ ion that is bound by the four nitrogen atoms of the cyclen. The mean distances of Ag1–C (C15 and C37) and Ag1–C (C30 and

Received: July 4, 2014
Published: September 23, 2014

   dx.doi.org/10.1021/ic501590a | *Inorg. Chem.* 2014, 53, 10514–10519

Scheme 1

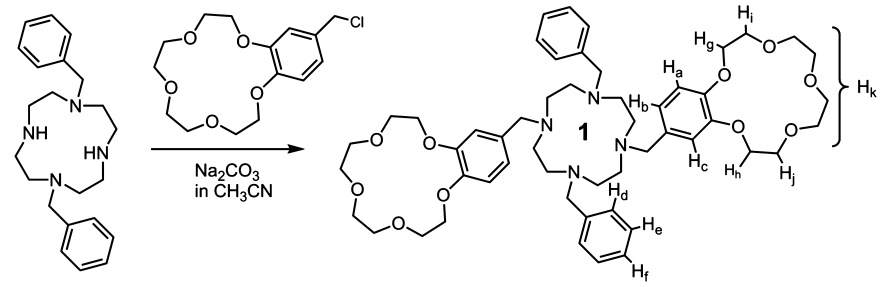

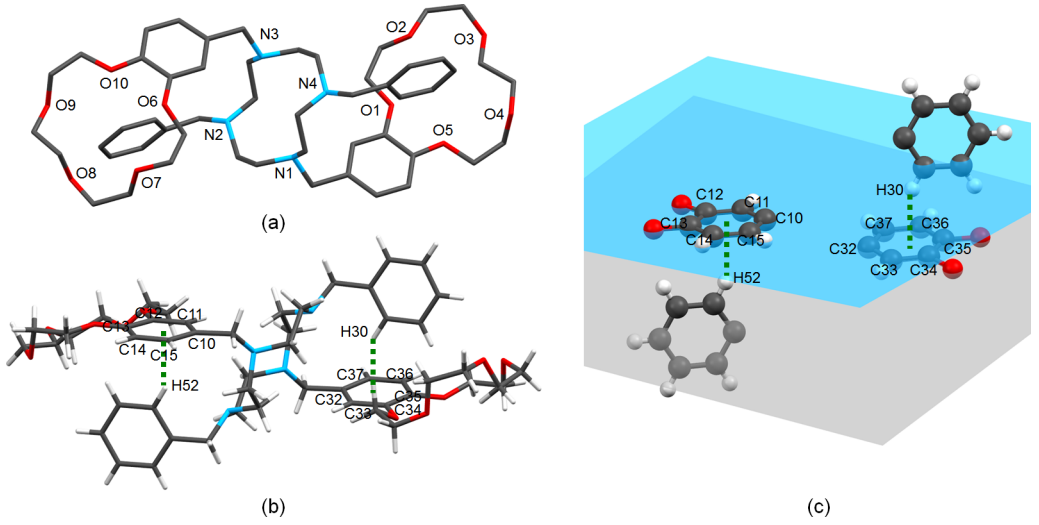

Figure 1. X-ray structure of **1**. Top view without hydrogen atoms (a) and side view with hydrogen atoms (b). Partial view for aromatic rings (c). Horizontal blue and gray planes are the mean planes through the atoms C10−C15 and C32−C37, respectively. Green dotted lines show the shortest distances between the benzene rings and the hydrogen atoms of the nearest neighbor benzenes. Solvent atoms are omitted for clarity.

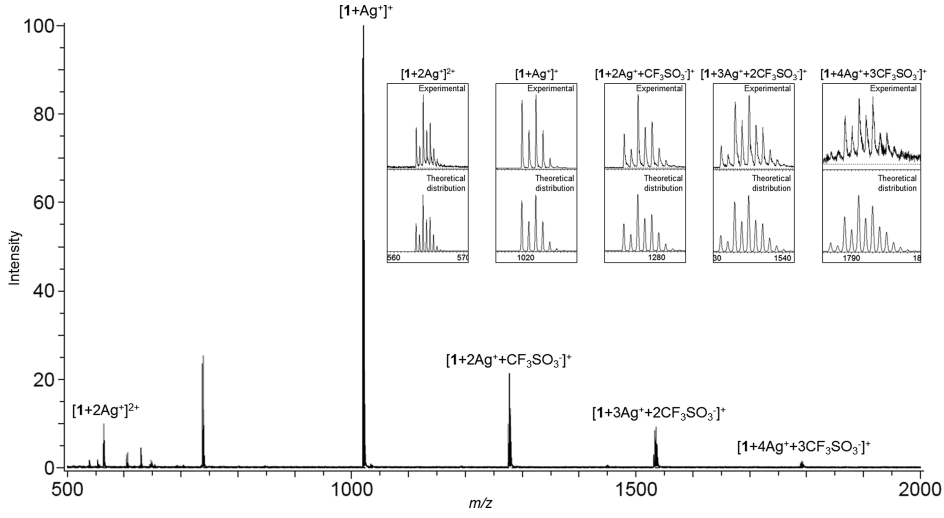

Figure 2. CSI-MS of a 1:3 mixture (**1**/Ag^+) in methanol (298 K).

C52) are 3.5535 and 3.005 Å, respectively. The crystallographic structure also suggests that the Ag−C (aromatic rings) distances are dependent on the electron densities on the benzene rings, as expected from the electrostatic potential maps (Figure S7 in the Supporting Information). The distances between the hydrogen atoms at the 2′ and 6′ positions of the side arms and the adjacent benzene planes are in the range of 2.594−2.643 Å. These distances are also typical CH−π bond distances.[2] Two crown ether rings are positioned at opposite sides.

The structure of the **1**·Ag^+ complex in solution was confirmed by Ag^+-induced ^{1}H NMR chemical shift changes. As shown in Figure 4, when 1 equiv of Ag^+ was added, the H_b (brown ◇), H_c (orange ○) protons of the benzo-15-crown-5 units, and the H_d (red ▲) protons at the 2′ and 6′ positions of the phenyl groups, shifted to higher field by ca. 1.24, 0.27, and

dx.doi.org/10.1021/ic501590a | Inorg. Chem. 2014, 53, 10514−10519

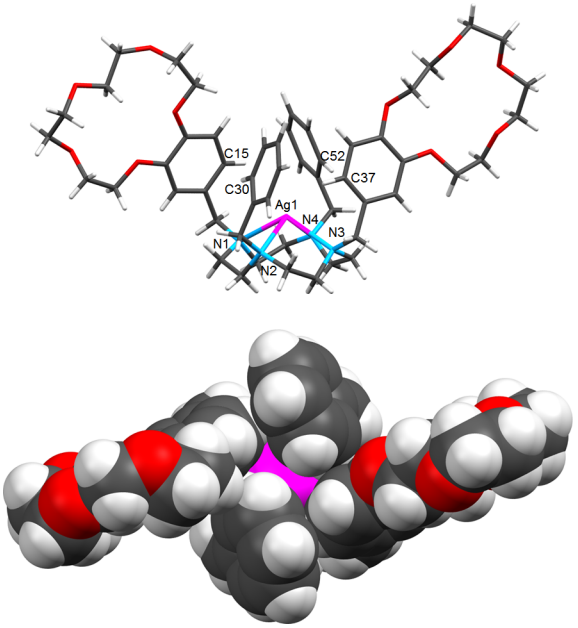

Figure 3. X-ray structure of **1**·$AgCF_3SO_3$ complex. (upper) Side view, tube model and (lower) top view, space-filling model.

0.65 ppm, respectively. These chemical shift changes indicate that the protons at the 2′ and 6′ positions of the aromatic side arms are located in the shielding area of the adjacent aromatic rings. Upon the addition of an excess amount of Ag^+ ([Ag^+]/[**1**] = 1.5−3.0), significant downfield shifts were observed in the proton signals of the crown moiety (H_g−H_k). These chemical shift changes indicate that the two benzo-15-crown-5 ethers also bind Ag^+ in the presence of excess Ag^+. Under these conditions, the H_b, H_c, and H_d protons at the 2′ and 6′ positions in the aromatic side arms retain their higher field shift. Interestingly, when 2 equiv of [2.2.2]cryptand were added to the 1:3 (= **1**/Ag^+) mixture, the chemical shifts of the protons on the aromatic side arms and crown ethers reverted to values found for the 1:1 mixture (= **1**/Ag^+) conditions. It is known that the log K values of cyclen·Ag^+ (= 1:1),[12] benzo-15-crown-5·Ag^+ (= 1:1),[13] and [2.2.2]cryptand·Ag^+ (= 1:1)[14] complexes are 9.75, 3.98, and 12.22, respectively. The log K values support the results of the titration experiments. Titration experiments indicate that the aromatic side arms continue to cover the Ag^+, even though the benzo-15-crown-5 ethers in the side arms bind the Ag^+.

Figure 5 shows calculated electrostatic potential (ESP) maps of the X-ray structures of **1** and **1**·Ag^+ complex and a DFT-optimized structure of **1**·3Ag^+ complex (B3LYP/3-21G*).[11] The ESP maps indicate that the cyclen ring in the **1**·Ag^+ complex has less electron density on the aromatic and the cyclen rings than does **1**. As shown in Figure 5c, the blue color of the ESP map of the optimized **1**·3Ag^+ complex illustrates a significant low level of electron density. The results of ^{1}H NMR titration and the ESP maps, therefore, indicate that the aromatic rings in **1**·Ag^+ complex cover the Ag^+ incorporated in the cavity ligand even though the two crown ethers in the side arms bind Ag^+.

To estimate the log K values for the interaction between **1** and Ag^+, Ag^+-induced UV spectral changes were measured at 23 °C (Figure 6 and associated multimedia file). Nonlinear least-squares analyses of the titration profiles clearly indicated the formation of 1:1, 1:2, and 1:3 complexes (= **1**/Ag^+), and allowed us to estimate the association constants defined as eq 1.[15] As shown in Figure 7, the log K_{11}, log K_{12}, and log K_{13} values for the 1:1, 1:2, and 1:3 complexes are 9.4, 5.8, and 4.0, respectively, where, K_{11}, K_{12}, and K_{13} are defined as follows:

$$1 + Ag^+ \rightarrow 1{\cdot}Ag^+ \quad K_{11} = [1{\cdot}Ag^+]/[1][Ag^+] \tag{1}$$

$$\mathbf{1}{\cdot}Ag^+ + Ag^+ \rightarrow \mathbf{1}{\cdot}2Ag^+ \quad K_{12} = [\mathbf{1}{\cdot}2Ag^+]/[1{\cdot}Ag^+][Ag^+] \tag{2}$$

$$\mathbf{1}{\cdot}2Ag^+ + Ag^+ \rightarrow \mathbf{1}{\cdot}3Ag^+ K_{13} = [\mathbf{1}{\cdot}3Ag^+]/[\mathbf{1}{\cdot}2Ag^+][Ag^+] \tag{3}$$

The determined log K values are comparable with those of cyclen·Ag^+ [log K = 9.75 (25 °C) for the 1:1 complex][12] and benzo-15-crown-5·Ag^+ [log K = 3.98 (25 °C) for the 1:1 complex][13] systems.

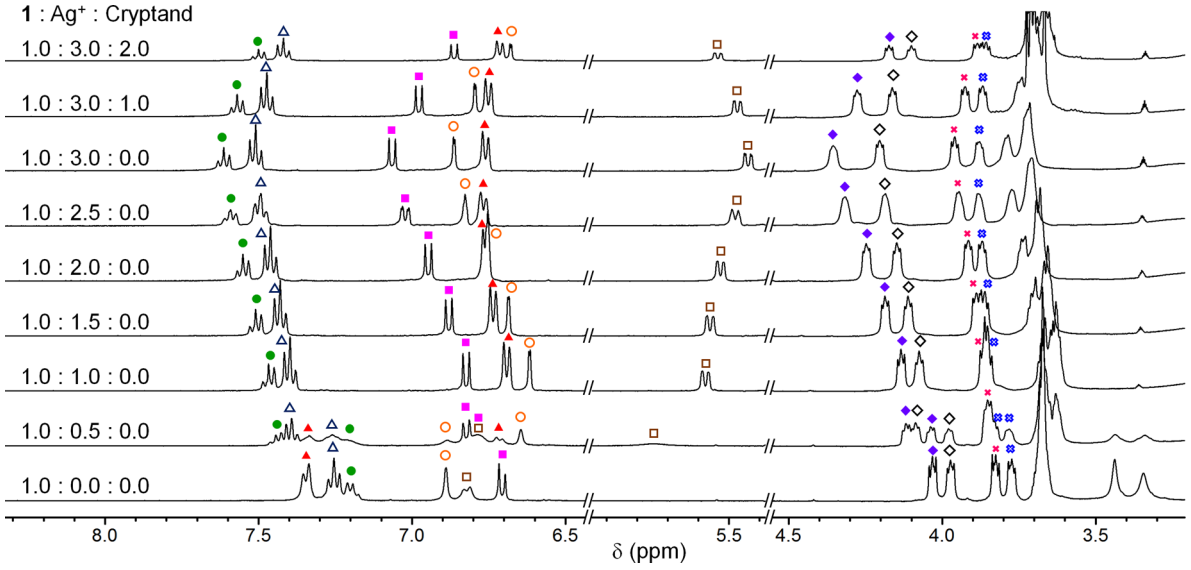

Figure 4. Ag^+-induced chemical shift changes of **1** (CD_2Cl_2/CD_3OD). After 3.0 equiv of Ag^+ were added to a 1:3 (= **1**/Ag^+) mixture, 1.0 and 2.0 equiv of [2.2.2]cryptand were added.

dx.doi.org/10.1021/ic501590a | Inorg. Chem. 2014, 53, 10514−10519

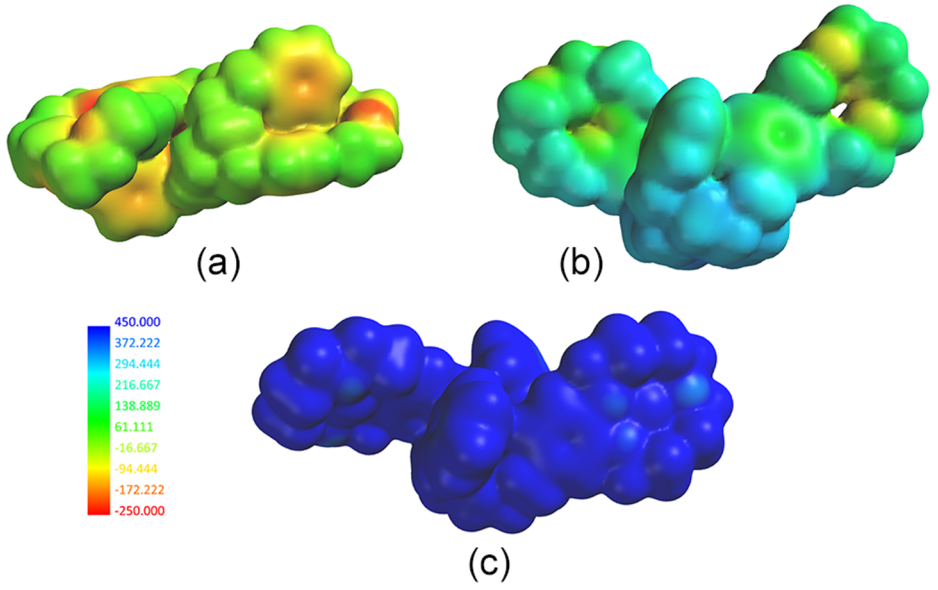

Figure 5. Electrostatic potential (ESP) maps of (a) **1**, (b) **1**·Ag^+ complex, and (c) **1**·3Ag^+ complex. The X-ray structures of **1** and **1**·Ag^+ complex were used as input coordinates to calculate the respective ESP maps. The structure of **1**·3Ag^+ complex was optimized using B3LYP/3-21G*.

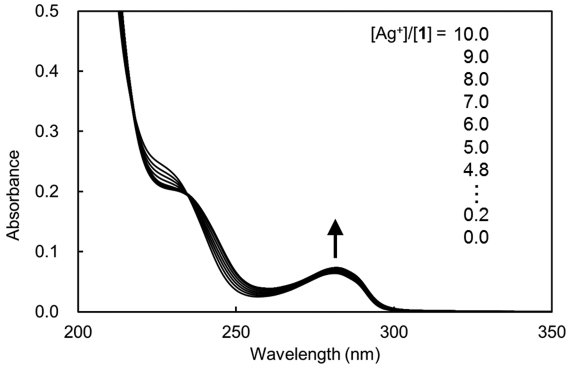

Figure 6. Ag^+-induced UV spectral changes of **1** in CH_3OH. [**1**] = 1.0 × 10^{-5} M.

Structures of the complexes of **1** with alkali metal ions in the absence and presence of Ag^+ in a solution were examined by ^1H NMR titration experiments. When Na^+ and K^+ were added to **1** in the absence of Ag^+, the ^1H NMR spectra broadened (see Figure S8a,b in the Supporting Information). These results suggest that intermolecular complexes (polymeric complexes) with alkali metal ions can be formed by a number of alkali metal cations and the ligands because **1** has two benzo-15-crown moieties. Conversely, sharp signals were observed in the Na^+ and K^+-induced spectral changes in the **1**·Ag^+ complex (Figure 8). As shown in the left-hand side of Figure 8, the H_g, H_h, H_i, and H_j proton signals of the crown ether moiety are shifted to the lower field by ca. 0.13−0.26 ppm upon addition of Na^+, and an inflection point was observed at 1.0:1.0:2.0 (= **1**/Ag^+/Na^+). However, when K^+ was added, the H_g, H_h, H_i, and H_j protons in the crown ether moiety show a different behavior [Figure 8 (right-hand side)]. In this case, signals for the H_g and H_h protons were split at 1.0:1.0:1.0 (= **1**/Ag^+/K^+), the H_i, H_j, and H_k protons shifted to higher field by ca. 0.1−0.05 ppm, and an inflection point was observed at 1.0:1.0:1.0 (= **1**/Ag^+/K^+).

These ^1H NMR data suggest (Figure 9) that (i) the **1**·Ag^+ complex forms a 1:2 (= **1**·Ag^+/Na^+) complex with Na^+, (ii) the conformation of the side arms (benzo-15-crown-5 moieties) in the **1**·Ag^+ complex rearrange to provide a suitable conformation for a 1:1 (= **1**·Ag^+/K^+) complex, and (iii) the benzo-15-crown-ether moieties in the **1**·Ag^+ complex do not form intermolecular complexes because of their bulkiness.[16] As shown in Figures S9 and S11 in the Supporting Information, the CSI-MS data of **1** and M^+ (M^+ = Na^+ and K^+) showed many fragment ions over a wide range. On the other hand, when Ag^+ was added (Figures S10 and S12 in the Supporting Information), the number of fragment ions decreased. The CSI-MS data support the ^1H NMR data.

In conclusion, we found that (i) the synthesized tetra-armed cyclen with crown ethers in the side arms behaves as an argentivorous molecule even though the crown ethers bind

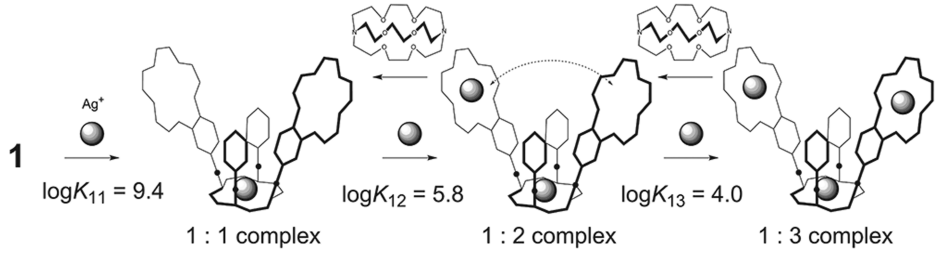

Figure 7. Schematic representation of the stepwise complexation of **1**·Ag^+. The dashed arrow in the 1:2 complex means an equilibrium between the two crown ether rings.

dx.doi.org/10.1021/ic501590a | Inorg. Chem. 2014, 53, 10514−10519

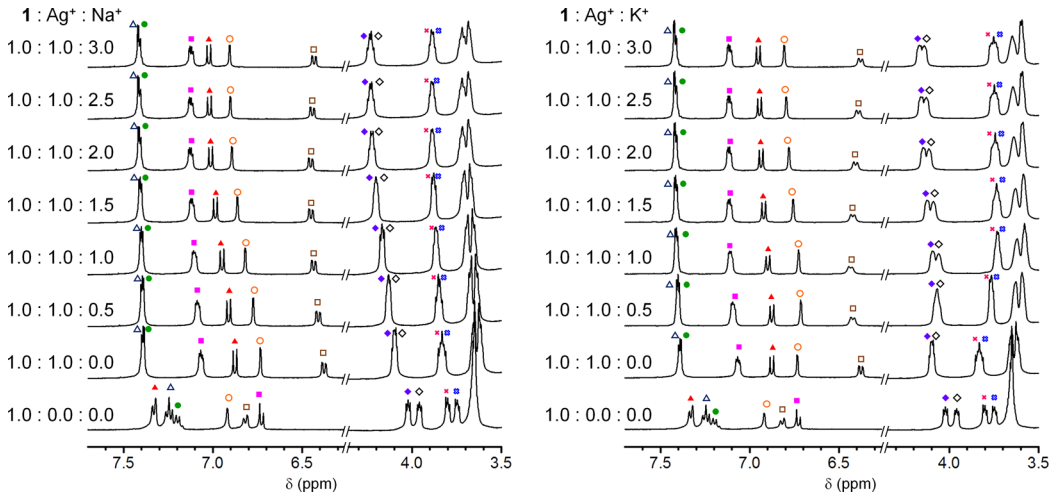

Figure 8. Na^+ (left) and K^+ (right) induced ^1H NMR spectral changes of the **1**·Ag^+ complex in CD_3CN/CD_2Cl_2 (1:1).

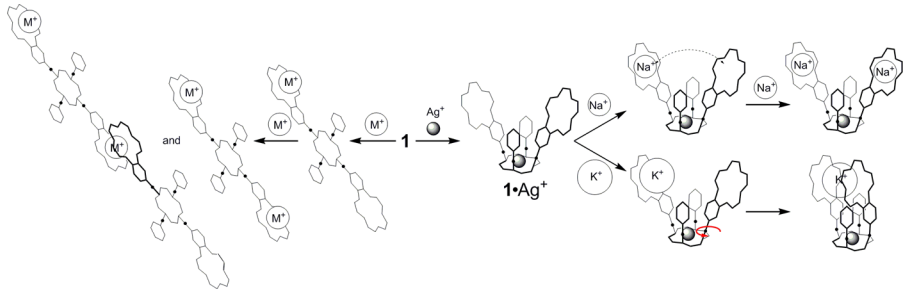

Figure 9. Schematic representations of structures of alkali metal complexes with **1** and **1**·Ag^+ complex.

metal cations, and (ii) the dynamic conformational changes of the aromatic side arms by forming the Ag^+ complex impact the binding properties of the crown ethers in the side arms toward alkali metal cations. The two crown ethers of **1** work cooperatively by forming a cyclen Ag^+ complex. By these findings, development of new functionalized argentivorous molecules is in progress in our laboratory.

EXPERIMENTAL SECTION

General Information. Melting points were obtained with a Mel-Temp capillary apparatus and were not corrected. FAB mass spectra were obtained using a JEOL 600 H mass spectrometer. ^1H NMR spectra were measured in $CDCl_3$ on a JEOL ECP400 (400 MHz) spectrometer. Cold ESI mass spectra were recorded on a JEOL JMS-T100CS mass spectrometer. All reagents were standard analytical grade and were used without further purification. 4′-chloromethylbenzo-15-crown-5 ether[9] and 1,7-bisbenzyl-1,4,7,10-tetraazacyclododecane[10c] were prepared according to the procedure described in the literature.

4′-Chloromethylbenzo-15-crown-5 ether. Na_2CO_3 (1.21 g, 8.75 mmol) was added to 4-hydroxymethyl benzo-15-crown-5 (0.902 g, 3.02 mmol) in anhydrous CH_2Cl_2 (50 mL), and the resulting mixture was cooled to 0 °C. Thionyl chloride (0.7 mL, 9.6 mmol) was added dropwise while under a dry nitrogen atmosphere, and the resulting reaction mixture was stirred for 12 h at room temperature. The reaction mixture was extracted with CH_2Cl_2 (2 × 30 mL) and then washed with H_2O (100 mL), saturated aqueous $NaHCO_3$ (100 mL), and H_2O (2 × 100 mL), before being dried (Na_2SO_4). The solvent was removed in vacuo to afford the crude product as a colorless oil in 90% yield (0.863 g). The crude product was used for subsequent steps without further purification because the product was almost one spot in a silica-gel thin-layer chromatography. ^1H NMR ($CDCl_3$): δ 7.01−6.75 (m, 3H), 4.54 (s, 2H), 4.22−4.05 (m, 4H), 3.98−3.84 (m, 4H), 3.76 (s, 8H). FAB-MS (m/z) (matrix: dithiothreitol (DTT)/α-thioglycerol (TG) = 1:1): m/z = 316 ($[M]^+$, 3%), 355 ($[M+K]^+$, 100%), 357 ($[M+K+2]^+$, 100%).

Synthesis of 1,7-Dibenzyl-4,10-bis(2,3,5,6,8,9,11,12-octahydro-1,4,7,10,13-benzopentaoxa-cyclopentadecin-15-ylmethyl)-1,4,7,10-tetraazacyclododecane (1). After stirring a mixture of 1,7-bis(3′,5′-difluorobenzyl)-1,4,7,10-tetraazacyclododecane (1.0 mmol) and aromatic aldehydes (4.1 mmol) in dry 1,2-dichloroethane (12 mL) at room temperature for 1 d under an argon atmosphere (1 MP), $NaBH(OAc)_3$ (4.0 mmol) was added, and the mixture was stirred for 1 d at room temperature. Saturated aqueous $NaHCO_3$ was added, and the aqueous layer was extracted twice with chloroform. The combined organic layer was washed with water, dried over Na_2SO_4, and concentrated. The residual solid was purified by column chromatography on silica gel. The main fraction was recrystallized from acetonitrile to give the following products. Mp: 51.1−53.0 °C. ^1H NMR (CD_2Cl_2): δ 7.44−7.15 (m, 10H), 7.01−6.65 (m, 6H), 4.14−3.91 (m, 8H), 3.89−3.73 (m, 8H), 3.73−3.59 (m, 16H), 3.43 (s, 4H), 3.33 (s, 4H), 2.66 (s, 16H). ^{13}C NMR ($CDCl_3$): δ 149.2, 148.2, 140.8, 133.7, 129.4, 128.4, 126.9, 121.8, 114.8, 113.8, 71.2, 71.17, 70.7, 70.6, 69.9, 69.8, 69.3, 69.0, 60.5, 60.1, 53.1, 53.0. FAB−MS (matrix: DTT/TG = 1:1): m/z = 915 ($[M]^+$, 10%), 916 ($[M+1]^+$, 20%). Anal. Calcd for $C_{52}H_{72}N_4O_{10}$+2/3H_2O: C, 67.51; H, 7.99; N, 6.06. Found: C, 67.40; H, 7.88; N, 6.05%.

Preparation of $AgCF_3SO_3$ Complex with 1 (1·$AgCF_3SO_3$). **1** (15 μmol) in chloroform (1 mL) was added to $AgCF_3SO_3$ (15 μmol) in methanol (1 mL). Crystals suitable for quantitative X-ray analysis were obtained upon evaporation of the solvent. **1**·$AgCF_3SO_3$. Mp (dec) > 200 °C. Anal. Calcd for $C_{53}H_{72}N_4F_3O_{13}SAg$: C, 54.40; H, 6.20; N, 4.79. Found: C, 54.05; H, 6.20; N, 4.70%.

^1H NMR Titration Experiments. ^1H NMR titration experiments were carried out at 298 K by the addition of $AgPF_6$ (1 mmol/μL) in CD_3OD to ligands (5 × 10^{-3} mmol/0.65 mL in CD_2Cl_2). A 1:1 mixture of CD_3OD and CD_2Cl_2 was used in the titration experiments using alkali metal ions.

dx.doi.org/10.1021/ic501590a | Inorg. Chem. 2014, 53, 10514−10519

UV−vis Titration Experiments. UV−vis titration experiments were carried out by addition of 0.1−2.0 equiv of $AgPF_6$ in CH_3CN (3.0×10^{-2} M) to ligands in CH_3CN (1.0×10^{-4} M, 3 mL) at 298 K.

X-ray Crystallography. Crystals of **1** and **1**·$AgCF_3SO_3$ were mounted atop a glass fiber, and data collections were performed using a Bruker SMART CCD area diffractometer at 173−273 K. Data were corrected for Lorentz and polarization effects, and absorption corrections were applied using the SADABS[17] program. Structures were solved by direct methods and subsequent difference-Fourier syntheses using the program SHELEX.[18] All non-hydrogen atoms were refined anisotropically, and hydrogen atoms were placed at calculated positions and then refined using $U_{iso}(H) = 1.2U_{eq}(C)$. The crystallographic refinement parameters of the complexes are summarized in Table 2.

Table 2. Crystal Data of 1 and 1·Ag CF_3SO_3

compound	1	1·$AgCF_3SO_3$
formula	$C_{54}H_{74}Cl_6N_4O_{10}$	$C_{55}H_{80}AgF_3N_4O_{15}S$
M	1151.87	1234.16
T/K	173 K	273 K
wavelength	0.71073	0.71073
crystal system	triclinic	triclinic
space group	$P\bar{1}$	$P\bar{1}$
a/Å	12.6301(8)	13.3083(9)
b/Å	13.5359(8)	14.7067(10)
c/Å	16.5061(10)	15.6790(10)
α (deg)	89.070(2)	79.7670(10)
β (deg)	84.4480(10)	73.1670(10)
γ (deg)	85.981(2)	76.7900(10)
U/Å^3	2801.6(3)	2839.0(3)
Z	2	2
D_c/g cm^{-3}	1.365	1.444
μ/mm^{-1}	0.367	0.472
data/restraints/parameters	13809/0/667	14935/2/724
number of reflns used [$>2\sigma(I)$]	[R(int) = 0.0272]	[R(int) = 0.0332]
R_1 ,wR_2 [$I > 2\sigma(I)$]	0.1294, 0.3520	0.0613, 0.1224
R_1, wR_2 [all data]	0.1890, 0.4009	0.0983, 0.1393
GOF	1.281	1.016

■ ASSOCIATED CONTENT

Ⓢ Supporting Information

CSI-MS, ^{1}H NMR, ^{13}C NMR, FAB-MS, and two-dimensional NMR data of **1** and **1**·Ag^+ complex. Crystallographic data of **1** and **1**·$AgCF_3SO_3$ (CIF). This material is available free of charge via the Internet at http://pubs.acs.org.

■ AUTHOR INFORMATION

Corresponding Author

*E-mail: habata@chem.sci.toho-u.ac.jp.

Notes

The authors declare no competing financial interest.

■ ACKNOWLEDGMENTS

This research was supported by Grants-in-Aid (08026969 and 11011761), a High-Tech Research Center project (2005−2009), and the Supported Program for Strategic Research Foundation at Private Universities (2012−2016) from the Ministry of Education, Culture, Sports, Science and Technology of Japan for Y.H.

■ REFERENCES

(1) Pedersen, C. J. *J. Am. Chem. Soc.* **1967**, *89*, 7017−36.
(2) We carried out the document retrieval using SciFinder, and more than 26 000 papers entitled "crown ether" were hit.
(3) Kohno, Y.; Shiraishi, Y.; Hirai, T. *J. Photochem. Photobiol., A* **2008**, *195*, 267−276.
(4) Benniston, A. C.; Gunning, P.; Peacock, R. D. *J. Org. Chem.* **2005**, *70*, 115−123.
(5) Tan, X.-Y.; Zhang, J.; Huang, Y.; Zhang, Y.; Zhou, L.-H.; Jiang, N.; Lin, H.-H.; Wang, N.; Xia, C.-Q.; Yu, X.-Q. *Chem. Biodiversity* **2007**, *4*, 2190−2197.
(6) Plush, S. E.; Gunnlaugsson, T. *Dalton Trans.* **2008**, 3801−3804.
(7) Gunnlaugsson, T.; Leonard, J. P. *Chem. Commun.* **2003**, 2424−2425.
(8) Bernier, N.; Esteves, C. V.; Delgado, R. *Tetrahedron* **2012**, *68*, 4860−4868.
(9) "Argentivorous" is different from "argentophilic". "Argentophilic" is used in the sense of Ag^+−Ag^+ interactions. (a) Constable, E. C.; Housecroft, C. E.; Kopecky, P.; Neuburger, M.; Zampese, J. A. *Inorg. Chem. Commun.* **2013**, *27*, 159−162. (b) Luo, G.-G.; Wu, D.-L.; Liu, L.; Wu, S.-H.; Li, D.-X.; Xiao, Z.-J.; Dai, J.-C. *J. Mol. Struct.* **2012**, *1014*, 92−96. (c) Santra, R.; Garai, M.; Mondal, D.; Biradha, K. *Chemistry* **2013**, *19*, 489−93. (d) Senchyk, G. A.; Bukhan'ko, V. O.; Lysenko, A. B.; Krautscheid, H.; Rusanov, E. B.; Chernega, A. N.; Karbowiak, M.; Domasevitch, K. V. *Inorg. Chem.* **2012**, *51*, 8025−8033. (e) Stephenson, A.; Ward, M. D. *Chem. Commun.* **2012**, *48*, 3605−3607. (f) Xu, J.; Gao, S.; Ng, S. W.; Tiekink, E. R. T. *Acta Crystallogr., Sect E: Struct Rep. Online* **2012**, *68*, m639−40. (g) Xu, J.; Gao, S.; Ng, S. W.; Tiekink, E. R. T. *Acta Crystallogr., Sect. E: Struct. Rep. Online* **2012**, *E68*, m639−m640. (h) Yang, G.; Baran, P.; Martinez, A. R.; Raptis, R. G. *Cryst. Growth Des.* **2013**, *13*, 264−269.
(10) (a) Habata, Y.; Yamada, S. *J. Inclusion Phenom. Macrocyclic Chem.* **2004**, *49*, 17−20. (b) Habata, Y.; Ikeda, M.; Yamada, S.; Takahashi, H.; Ueno, S.; Suzuki, T.; Kuwahara, S. *Org. Lett.* **2012**, *14*, 4576−4579. (c) Habata, Y.; Taniguchi, A.; Ikeda, M.; Hiraoka, T.; Matsuyama, N.; Otsuka, S.; Kuwahara, S. *Inorg. Chem.* **2013**, *52*, 2542−2549. (d) Habata, Y.; Oyama, Y.; Ikeda, M.; Kuwahara, S. *Dalton Trans.* **2013**, *42*, 8212−8217. (e) Habata, Y.; Okeda, Y.; Ikeda, M.; Kuwahara, S. *Org. Biomol. Chem.* **2013**, *11*, 4265−4270.
(11) *Spartan '10;* Wavefunction, Inc.: Irvine, CA, 2011.
(12) Kira, J.; Niedzialkowski, P.; Ossowski, T. *J. Coord. Chem.* **2013**, *66*, 1220−1227.
(13) Izatt, R. M.; Terry, R. E.; Nelson, D. P.; Chan, Y.; Eatough, D. J.; Bradshaw, J. S.; Hansen, L. D.; Christensen, J. J. *J. Am. Chem. Soc.* **1976**, *98*, 7626−7630.
(14) Buschmann, H.-J. *Inorg. Chim. Acta.* **1985**, *102*, 95−98.
(15) The log K values of the Ag+ complexes were calculated with the HypSpec program version 1.1.33. Gans, P.; Sabatini, A.; Vacca, A. *Talanta* **1996**, *43*, 1739−1753.
(16) Casnati, A.; Pochini, A.; Ungaro, R.; Bocchi, C.; Ugozzoli, F.; Egberink, R. J. M.; Struijk, H.; Lugtenberg, R.; de, J. F.; Reinhoudt, D. N. *Chem.—Eur. J.* **1996**, *2*, 436−445.
(17) *SADABS, version 2.03*;Sheldrick, G. M. Program for adsorption correction of area detector frames, Bruker AXS, Inc.: Madison, WI, 1996.
(18) *SHELXTL, version 5.1;* Bruker AXS, Inc.: Madison, WI, 1997.